

Finding Thermodynamically Favorable Pathways in Reaction Networks using Flows in Hypergraphs and Mixed Integer Linear Programming

Aditya Pal,^{*} Rolf Fagerberg,[†] and Jakob Lykke Andersen[‡]

*Department of Mathematics and Computer Science,
University of Southern Denmark,
Campusvej 55, 5230 Odense M, Denmark.*

Christoph Flamm[§]

*Department of Theoretical Chemistry, University of Vienna
Währinger Straße 17, 1090 Wien, Austria.*

Peter Dittrich[¶]

*Department of Mathematics and Computer Science,
Friedrich Schiller University Jena
Fürstengraben, 07743, Jena, Germany.*

Daniel Merkle^{**}

*Faculty of Technology, Bielefeld University,
Postfach 10 01 31, 33501 Bielefeld, Germany
and
Department of Mathematics and Computer Science,
University of Southern Denmark,
Campusvej 55, 5230 Odense M, Denmark.*

(Dated: November 26, 2024)

Abstract

Finding pathways that optimize the formation of a particular target molecule in a chemical reaction network is a key problem in many settings, including reactor systems. Reaction networks are mathematically well represented as hypergraphs, a modeling that facilitates the search for pathways by computational means. We propose to enrich an existing search method for pathways by including thermodynamic principles. In more detail, we give a mixed-integer linear programming (mixed ILP) formulation of the search problem into which we integrate chemical potentials and concentrations for individual molecules, enabling us to constrain the search to return pathways containing only thermodynamically favorable reactions. Moreover, if multiple possible pathways are found, we can rank these by objective functions based on thermodynamics. As an example of use, we apply the framework to a reaction network representing the HCN-formamide chemistry. Alternative pathways to the one currently hypothesized in literature are queried and enumerated, including some that score better according to our chosen objective function.

CONTENTS

I. Introduction	4
A. Context and Motivation	4
B. Previous Work	5
C. Our Contribution	6
D. Paper Structure	6
II. Definitions	7
A. Directed Hypergraphs	7
B. Integer Hyperflows	8
III. Methods	10
A. Mathematical Formulation	11
1. Constraint-Based Model	12
2. Objective Function	14

* adpal@imada.sdu.dk

† rolf@imada.sdu.dk

‡ jlandersen@imada.sdu.dk

§ xtof@tbi.univie.ac.at

¶ peter.dittrich@uni-jena.de

** daniel.merkle@uni-bielefeld.de

3. Temporal Ordering of Molecules	15
B. Implementation	15
1. Implementing the Objective function	16
2. Linearizing the Constraints	16
C. Implemented Model	18
D. Thermodynamic Oracle	21
IV. Results	21
V. Discussion	25
VI. Conclusion	27
References	29
A. Appendices	33
1. On assigning the Chemical Potentials	33
2. On the range of the concentration variable	34
3. Graph Transformation rules used	35

I. INTRODUCTION

Equilibrium thermodynamics has been often used to determine the spontaneity of an isolated chemical reaction. Specifically, from the Gibbs free energy one can find the driving forces behind a reaction and determine whether its occurrence is favorable or not. However, in practical scenarios, reactions are seldom encountered in isolation. Rather, they are components of larger interconnected networks, where the products of one reaction may be the reactants of numerous other reactions. Such networks are called *reaction networks*. In this paper, an existing computational methodology for searching for pathways in reaction networks via flow queries is extended with the ability to include equilibrium thermodynamics among the search constraints.

A. CONTEXT AND MOTIVATION

Reaction networks are recurrent in real-world scenarios: cellular metabolic processes, interactions among atmospheric constituents, environmental phenomena like cycling of nutrients and pollutants, the human gut microbiome, and industrial chemical reactors. Modeling these networks is challenging due to the inherent complexities of such systems. One type of complexity arises from nonlinear dynamics, which appear in particular when transcending one-to-one reactions. Another type of complexity arises from the existence of parallel and alternative sequences of reactions, termed pathways, which may give the same overall effect but involve distinct yet intersecting sets of molecules. Such pathways are manifested in diverse contexts: metabolic pathways in organisms for cellular metabolic networks, nutrient cycles in the environment, and synthesis plans in chemical reaction networks.

The exploration of reaction networks to synthesize molecules has primarily been done experimentally in the wet laboratory. However, this process is labor-consuming, cost inefficient and limits the pace of exploration. *In silico* modeling and exploration of reaction networks have the potential to speed up the process and guide manual efforts. The finer the physical details included in the modeling of the reaction networks, the more accurate the results can be expected to be. The ultimate way of doing that would be to construct the complex free energy landscape for the full reaction network, which then, in principle, would allow for the full simulation of reactions, as these are ultimately guided by the laws of thermodynamics. However, we believe that this is currently past any modeling and computational capacities available. A first and more realistic step towards the goal is using chemical potentials to determine if a given reaction is favorable in thermodynamical terms, and then use only the favorable reactions in the exploration of the reaction networks.

B. PREVIOUS WORK

Values derived from thermodynamics have been used to suggest pathways in reaction networks through pathfinding algorithms and a linear combination of the lowest cost paths in that network in [1]. In thermodynamics-based metabolic flux analysis [2], the mass balance constraints of metabolic flux analysis are augmented by additional thermodynamic constraints, to produce flux distributions and metabolite activity profiles free from thermodynamic infeasibilities. Nonequilibrium thermodynamics was developed to explore reaction networks, employing a stochastic trajectory-based approach to define energy, entropy, and heat dissipation along reactions in [3]. Building upon stochastic thermodynamics, a nonequilibrium thermodynamic framework for open reaction networks has been formulated in [4], governed by deterministic rate equations with mass action kinetics and introducing a nonequilibrium Gibbs free energy quantifying the minimal work required to induce nonequilibrium states from an equilibrium state. This nonequilibrium Gibbs free energy is minimized as the open detailed-balanced network relaxes to an equilibrium state, aligning with the maximum entropy principle. The application of ‘circuit theory’ to reaction networks [5] extends the chemical analogs of Kirchhoff’s laws for predicting reaction currents within complex reaction networks. Previous studies also utilize linear programming to identify complex balanced realizations of mass action kinetics in reaction networks [6]. Works have introduced numerical procedures for determining weakly reversible chemical reaction networks using integer linear programming (ILP), emphasizing the significance of ILPs in identifying specific network properties [7–9]. Mixed-integer linear programming (MILP) has been employed to prune chemical reaction networks using experimental data, demonstrating the application of MILP in understanding complex chemical systems [10].

Much of the work cited in the preceding paragraph primarily focuses on theoretical formulations, with few executable implementations. In contrast, MØD [11] is a software package developed for generating and analyzing reaction networks [12, 13]. In the generative part of MØD, molecules are modeled by undirected graphs with attributes, hence with each atom explicitly represented [12], and reactions are modeled by rules for transforming molecule graphs. Reaction networks can automatically be generated from a set of rules and a set of starting molecules by using the graph transformation engine of MØD [14]. The outcome is a directed multi-hypergraph representing the reaction network. In the analysis part, queries for pathways in such reaction networks can then be specified using integer hyperflows as a formal model [15, 16] and the reaction network can be queried by computational means for the presence of the specified pathway. This framework thus allows a flexible, yet precise specification of pathways and a search for such pathways by computational means. However, the methodology [15] currently does not incorporate any dynamics in the modeling of the reaction network.

C. OUR CONTRIBUTION

In this paper, we incorporate thermodynamic principles into the existing hyperflow model in MØD. In particular, we develop methods based on mixed integer linear programming (MILP) that allow thermodynamic constraints to be added to the specification of pathways when searching for these in the MØD framework. Our methods can return several alternative pathways and these can be ranked on the basis of thermodynamic-based metrics.

We note that returning multiple pathways can significantly increase the practical value of the investigations: Models of reaction networks and estimations of thermodynamic parameters inherently are simplifications of reality, hence any single pathway returned may turn out to be less desirable in the face of further details of the chemical situation. Hence, having a number of highly ranked pathways available from which the practitioner can choose is a more robust strategy.

In our method, we need to assign chemical potentials to the molecules in the reaction network in order to calculate the Gibbs free energies for its reactions. In the current implementation, we use the semi-empirical method GFN2-xTB [17], which provides a good balance between the accuracy of the thermodynamic parameters and the ability to handle larger molecules. However, it can be replaced by any other method to assign the chemical potentials if the user desires so. For generality, we will refer to the chosen method as the thermodynamic oracle. We note that using a thermodynamic oracle to calculate the chemical potentials of the molecules in an automated fashion has the added benefit of being applicable in rule-based generative systems where the chemical space is expanded on the fly and the molecules generated are unknown at the start.

To the best of our knowledge, there currently does not exist a computational method for searching for pathways in reaction networks based on thermodynamic constraints that combines MILP with the wide applicability and speed of semi-empirical tight binding methods. In Section V, we give further details of the comparison of our work with existing frameworks.

D. PAPER STRUCTURE

The rest of this paper is organized as follows. In Section II, we give the definitions underlying our modeling of reaction networks and pathways. In Section III, which constitutes the core part of the paper, we give the details of our methods. In Section IV, we demonstrate the usability of the methods by applying them on a reaction network involving *H*CN. In Section V, we give the abovementioned comparison with some existing frameworks. In Section VI we offer a conclusion to the paper. Some additional technical details and discussions we have placed in appendices.

II. DEFINITIONS

In this section, we present our model for reaction networks and pathways, namely directed hypergraphs and integer hyperflows, respectively. This section is based on previous work in [12] and [15].

A. DIRECTED HYPERGRAPHS

A reaction network consists of set of molecules V and a set of reactions E . Each reaction $e \in E$ is generally a many-to-many mapping of molecules, which can be written [18] as the formal sum

$$\sum_{v \in V} s_{ve}^- v \longrightarrow \sum_{v \in V} s_{ve}^+ v$$

where s_{ve}^- and s_{ve}^+ denote the stoichiometric coefficients, i.e., the number of molecules of v that are used, respectively produced, by reaction e . The sum is over the entire set of molecules V in the reaction network, and for molecules v that do not take part in a particular reaction e , we have $s_{ve}^- = s_{ve}^+ = 0$. Hence, a reaction network is formally well represented [15] as a directed multi-hypergraph (V, E) , where the set V of vertices models molecules and the set E of directed multi-hyperedges models reactions. A directed multi-hyperedge $e \in E$ is an ordered pair (e^-, e^+) of multisets of vertices. The elements of e^- model the reactants of the reaction, with each reactant v appearing s_{ve}^- times, and correspondingly e^+ and s_{ve}^+ model the products of the reaction (we remark that the use of $+$ and $-$ is swapped compared to the notation in [15]). Figure 1 depicts a hypergraph with eight vertices and eleven hyperedges. As examples, hyperedge $e_0 \equiv (\{v_0\}, \{v_1\})$ represents the one-to-one reaction $v_0 \rightarrow v_1$, hyperedge $e_3 \equiv (\{v_0, v_1\}, \{v_3\})$ represents the many-to-one reaction $v_0 + v_1 \rightarrow v_3$, hyperedge $e_2 \equiv (\{v_2, v_2\}, \{v_1\})$ represents the many-to-one reaction $2v_2 \rightarrow v_1$, hyperedge $e_4 \equiv (\{v_3\}, \{v_0, v_1\})$ represent the one-to-many reaction $v_3 \rightarrow v_0 + v_1$, hyperedge $e_7 \equiv (\{v_3\}, \{v_5, v_5\})$ represent the one-to-many reaction $v_3 \rightarrow 2v_5$, and hyperedge $e_9 \equiv (\{v_3, v_4\}, \{v_7, v_8\})$ represents the many-to-many reaction $v_3 + v_4 \rightarrow v_7 + v_8$.

On a related note, standard usage of the term ‘reaction’ implies the breaking and forming of chemical bonds. However, physical processes that do not alter the set of bonds in a molecule yet involve energy transformations, thereby affecting the molecule’s ability to participate in a reaction. For instance, some reactions occur only when a molecule is excited into a higher energy state, or certain molecules (such as phosphorus or sulfur) are in specific phases. Although such transitions are not conventionally termed ‘reactions,’ they are elementary processes accompanied by a change in free energy. Consequently, in the rest of this paper we will use the term ‘transition’ instead of ‘reaction’ to denote this broader set of relations between classes of molecules.

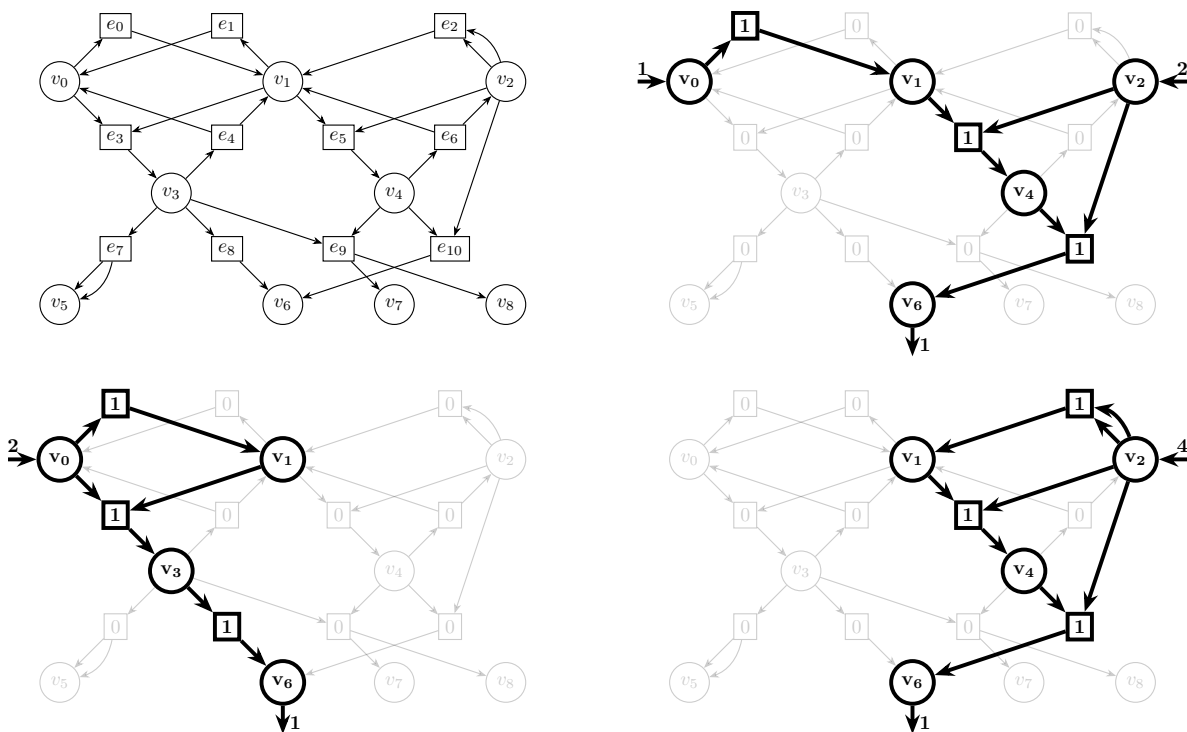


FIG. 1. A directed hypergraph (top-left), where circles are vertices and the squares are hyperedges. The other three figures show possible integer hyperflows in the hypergraph, each representing a pathway, where hyperedges with non-zero flow are drawn in bold. The inflow and the outflow are depicted as arrows in and out of the source and target vertices of the pathway. Hyperedges with multiple copies of a vertex as source or target are depicted with parallel arrows. See for instance e_7 , which has v_5 twice as a target and thus represents the reaction $v_3 \rightarrow 2v_5$.

B. INTEGER HYPERFLOWS

A pathway is a set of transitions that transforms some available source molecules into desired target molecules. To model pathways formally, [15] introduced the concept of an *integer hyperflow* f in a hypergraph $\mathcal{H} = (V, E)$, which we now explain.

A pathway is viewed as a vector $f_E \in \mathbb{N}_0^{|E|}$, i.e., an assignment of a non-negative integer to each edge in E , denoting how many times the corresponding transition appears in the pathway. Additionally, two vectors $f_{\text{in}} \in \mathbb{N}_0^{|V|}$ and $f_{\text{out}} \in \mathbb{N}_0^{|V|}$ denote for each molecule in V the amount of it consumed as source molecule, respectively produced as target molecule, by the pathway.

We want the pathway’s net effect on the number of molecules in the system to be specified entirely

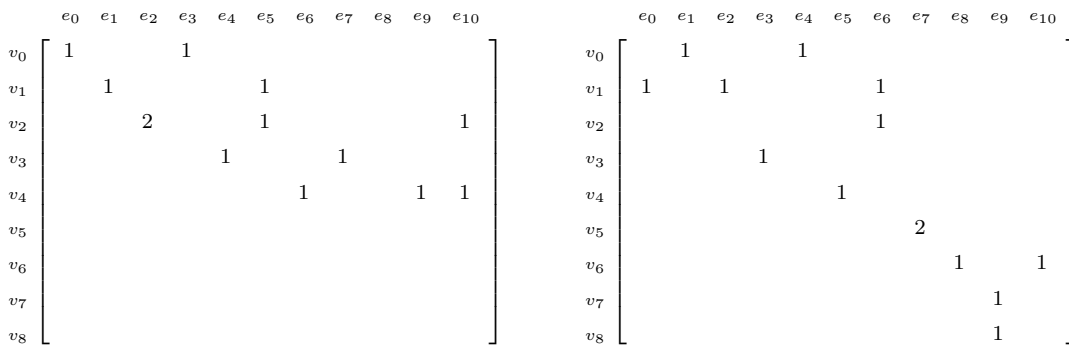


FIG. 2. A representation of the hypergraph from Figure 1 as an out-incidence matrix \mathbf{S}^- (left) and an in-incidence matrix \mathbf{S}^+ (right). Only non-zero entries are shown. Since the hypergraph has 9 vertices and 11 hyperedges, the matrices have dimensions 9×11 .

by f_{in} and f_{out} .

$$\mathbf{S}^+ \cdot f_E - \mathbf{S}^- \cdot f_E = f_{\text{out}} - f_{\text{in}} \quad (1)$$

where \mathbf{S}^- is a $|V| \times |E|$ matrix with entries s_{ve}^- and \mathbf{S}^+ is a $|V| \times |E|$ matrix with entries s_{ve}^+ (recall from Section II A that s_{ve}^- and s_{ve}^+ are the numbers of molecule v consumed and produced by reaction e). In hypergraph terminology, \mathbf{S}^- and \mathbf{S}^+ are the out-incidence matrix and the in-incidence matrix, respectively.¹ The matrices \mathbf{S}^- and \mathbf{S}^+ for the hypergraph in Figure 1 are shown in Figure 2.

To unify the three vectors f_E , f_{in} , and f_{out} into a single flow vector on hyperedges, the authors of [15] introduce for each $v \in V$ two so-called half-edges $e_v^+ = (\emptyset, v)$ and $e_v^- = (v, \emptyset)$. These represent the production of v as source molecule addition to the system and the consumption of v as target molecule removal from the system, respectively. Setting

$$\begin{aligned} E^+ &= \{e_v^+ \mid v \in V\} \\ E^- &= \{e_v^- \mid v \in V\} \\ \overline{E} &= E \cup E^+ \cup E^-, \end{aligned}$$

the authors of [15] introduce the extended hypergraph $\overline{\mathcal{H}} = (V, \overline{E})$ and define an *integer hyperflow* to be a vector $f \in \mathbb{N}_0^{|\overline{E}|}$ satisfying the flow conservation constraint

$$\forall v \in V: \sum_{e \in \overline{E}} s_{ve}^+ f_e - \sum_{e \in \overline{E}} s_{ve}^- f_e = 0 \quad (2)$$

¹ In other settings, \mathbf{S}^- and \mathbf{S}^+ are called the reactant stoichiometric matrix and the product stoichiometric matrix. One can also meet a single stoichiometric matrix, defined as $\mathbf{S} = \mathbf{S}^+ - \mathbf{S}^-$. This latter version is less expressive for reaction network modeling, as the role of catalysts and autocatalytic molecules cannot be captured. In some contexts, f_{in} and f_{out} are called the external compounds.

Here, s_{ve}^- is an entry in the $|V| \times |\overline{E}|$ out-incidence matrix of $\overline{\mathcal{H}}$, s_{ve}^+ is an entry in the $|V| \times |\overline{E}|$ in-incidence matrix of $\overline{\mathcal{H}}$, and f_e is an entry in f . The constraint in Equation (2) is easily seen to be equivalent to the constraint in Equation (1). A detailed discussion of how integer hyperflows relate to, and differ from, other similar concepts such as elementary modes, extreme pathways, and flux balance analysis can be found in Section 2.6 of [15].

In Figure 1, three possible hyperflows in a hypergraph are depicted. Unboxed integers are flow values on half-edges, while boxed integers are the flow values for hyperedges in E . For clarity, only half-edges with non-zero flow values are shown.

One key feature of integer hyperflows is that they give a flexible and generic way to *specify* pathways via constraints on the flow on half-edges. This may be as straight-forward as specifying an overall reaction for the pathway by fixing the flow on the half-edges for the molecules in the source and target sets and setting the flow to zero for the rest of the half-edges. Or one may specify upper and lower limits for some half-edges and free values for others, for instance to ask if there is any way to produce at least some target molecules using any amount of source molecules, while at the same time allowing waste products.

Then a *search* for pathways fulfilling the specification amounts to finding flow vectors f obeying those constraints, in addition to the constraint in Equation (2). Since integer hyperflows are integer valued, it is natural to model the situation via the ILP formalism and search for f using an ILP solver. This idea has been implemented as part of the software system MØD [11]. The result is a powerful and flexible tool for specifying and searching for pathways (integer hyperflows) in a given chemical reaction network (hypergraph). The flexibility is further increased by the possibility of having flow values in the ILP objective function, such that e.g. flow solutions allowing but minimizing waste can be found. Also the flow values on non-half-edges can enter the specification and/or optimization, allowing e.g. the search for solutions minimizing the use of a given transition deemed particularly expensive to include in the pathway.

III. METHODS

We would like to incorporate elements from thermodynamics to refine the existing search query for pathways in reaction networks. Analogous to typical thermodynamics problems where pathways maximizing the work done by the flow of heat between the system and the reservoir are sought (such as the cycle of a heat engine), we seek pathways in our system to maximize the chemical work done (interpreted as maximizing the production of the target molecules) by directing the flow of molecules along specific transitions on the free energy landscape.

Classical thermodynamics—contrary to the ‘dynamics’ in the name—is used to study systems at equilibrium, or near equilibrium, when the thermodynamic driving forces are in exact balance. In a closed system, the concentrations of the molecules in the system would be such that the chemical potentials of all the molecules in the reaction network is the same. To achieve the required flow along the pathway returned by our method, one has to perturb the system from the equilibrium by tweaking the molecular concentrations in a direction returned by the solution. In practical scenarios, this is done supplying a steady inflow of the source molecules and removing the target molecules from the system to maintain a non-zero thermodynamic driving force along the pathway. For perturbations that are small enough, the equations from classical thermodynamics describing the equilibrium situation can still be used as a first-order approximation. The gradients of the chemical potentials in general, or in our case, the differences in the chemical potentials of the target molecules and the source molecules in an elementary transition serve as the thermodynamic force driving a transition. In the linear regime, the flow for each transition would be directly proportional to the thermodynamic forces driving the flow. The forces driving the flows in a reaction network might not remain linear functions of the difference in the chemical potentials farther from the equilibrium, resulting in non-linear dynamics. Therefore, in this work we would restrict ourselves to analyzing the system perturbed, within acceptable limits, from the equilibrium, so that using equations from equilibrium thermodynamics does not introduce large errors into the calculations.

A. MATHEMATICAL FORMULATION

The first step to make the search more realistic is to assign the chemical potentials to the vertices and add constraints which allow only thermodynamically favorable transitions in the returned pathway. Chemical potentials are real-valued numbers. Hence, the inclusion of customized linear constraints and objective functions involving floating-point variables for the chemical potentials and concentrations of molecules requires us to extend the existing ILP model in MØD to one using MILP incorporating these variables. This is the key focus of the current work.

MILP attempts to model the system with linear inequalities involving some variables (both integer-values and floats, hence mixed) describing the system. An infeasible system of inequalities indicates that there is no solution to the problem under those specific constraints. When a feasible solution space exists, one often attempts to optimize the solution, by maximizing (or minimizing) the value of some objective function. In this section, we develop the structure of the MILP model, first with using logical constraints using implications in Section III A 1, and later, in Section III B, linearize it into an MILP that can be solved using a solver.

1. CONSTRAINT-BASED MODEL

Since we are extending the existing integer hyperflow formulation in [15], the base ILP formulation for modeling flow conservation in pathways in reaction networks is inherited from that work, as described in Section II B.

$$\forall v \in V: \sum_{e \in \bar{E}} s_{ve}^+ f_e - \sum_{e \in \bar{E}} s_{ve}^- f_e = 0 \quad (2)$$

Any set of integer flow values on \bar{E} induces some overall reaction, which corresponds to flow values on $E^+ \cup E^-$ that make Equation (2) hold. However, the set of available source molecules is often constrained by practical considerations such as cost, ease of availability and purity. Similarly, for the flow to be of practical utility, we could be interested in flows which maximize the outflow of a particular molecule, produce minimum side-products, and perhaps limit the use of particularly expensive reactions. As explained in Section II B, such conditions are modeled as constraints on the flow values f_e , in particular for e in E^+ and E^- , but potentially also in \bar{E} . These constraints constitute a structural specification of the pathway searched for:

$$\text{Structural specification constraints on } f_e \text{ for } e \in \bar{E} \quad (3)$$

To also incorporate thermodynamics into the modeling, we propose assigning a chemical potentials for each vertex v , $x_v^{G^0}$, under standard physical conditions, which are calculated using a thermodynamic oracle described in Section III D. The differences in the chemical potentials of the target set and the source set in a transition e , $x_e^{\Delta G}$, serve as the thermodynamic force driving the transition, dictating the direction of flow of matter along that hyperedge. In the linear regime, not far away from the equilibrium, the thermodynamic flows on a particular hyperedge is directly proportional to the thermodynamic force driving it. The difference in chemical potential for a transition can be manipulated by altering the concentrations of the molecules involved. We choose to represent the log concentration of a molecule v by the variable x_v^K . The nudged difference in chemical potentials for a transition e is represented as the variable, $x_e^{\Delta G}$ after taking into account the effect of the log concentration, x_v^K , of the molecules involved in the transition e . We would like to have an assignment of variables x_v^K (within practical limits) such that the pathway consists of transitions with only negative differences in chemical potentials, of in other words, thermodynamically favorable transitions. The variables in the MILP formulation are listed in Table V.

The flow f_e through a hyperedge e must be positive.

$$\forall e \in \bar{E}: 0 \leq f_e \quad (4)$$

Since the transitions are reversible, separate hyperedges are added for the forward and backward directions. Under specific physical conditions, thermodynamic forces dictates that either the forward or the backward direction of a reversible transition is more likely. The direction of the flow is in the direction in which the difference in chemical potential for a hyperedge e , $x_e^{\Delta G}$, is negative. The following implication-based constraint ensures that the pathway returned by the MILP solver consists of thermodynamically favorable transitions only.

$$\forall e \in E: f_e > 0 \implies x_e^{\Delta G} \leq 0 \quad (5)$$

The difference in chemical potential, $x_e^{\Delta G}$ under arbitrary log concentration values, x_v^K of the molecules participating in the transition e is calculated from the difference in chemical potential under standard conditions, $x_v^{G^0}$, by the following equations.

$$\begin{aligned} \forall e \equiv (e^-, e^+) \in E: \\ x_e^{\Delta G} = \left(\sum_{v \in e^+} x_v^{G^0} - \sum_{v \in e^-} x_v^{G^0} \right) + RT \cdot \left(\sum_{v \in e^+} x_v^K - \sum_{v \in e^-} x_v^K \right) \end{aligned} \quad (6)$$

The molecules on the left side and right side of an elementary transition belong to e^- and e^+ respectively. R is the universal gas constant (in appropriate units) while T is the absolute temperate of the system. Therefore, RT is a constant for the system. The log concentration of the molecules, x_v^K , is allowed to vary within a range $[x_v^K]_{\min} \leq x_v^K \leq [x_v^K]_{\max}$, set by practical and physical constraints detailed in Appendix A2, to mimic the conditions inside a reactor.

$$[x_v^K]_{\min} \leq x_v^K \leq [x_v^K]_{\max} \quad (7)$$

Note that the dependence of difference in the chemical potentials for a transition e on the concentrations of the molecules involved is not linear.

$$\begin{aligned} x_e^{\Delta G} &= x_e^{\Delta G^0} + RT \ln \left(\frac{\prod_{v \in e^+} \text{conc}(v)}{\prod_{v \in e^-} \text{conc}(v)} \right) \\ &= x_e^{\Delta G^0} + \frac{RT}{\ln 10} \left(\log \left(\prod_{v \in e^+} \text{conc}(v) \right) - \log \left(\prod_{v \in e^-} \text{conc}(v) \right) \right) \\ &= x_e^{\Delta G^0} + \frac{RT}{\ln 10} \left(\sum_{v \in e^+} \log \text{conc}(v) - \sum_{v \in e^-} \log \text{conc}(v) \right) \\ x_e^{\Delta G^0} &= \sum_{v \in e^+} x_v^{G^0} - \sum_{v \in e^-} x_v^{G^0} \end{aligned}$$

However, it can be represented as a linear expression, if one chooses to represent the log concentrations of the corresponding molecule v , $\log_{10} \text{conc}(v)$, as a variable x_v^K , in the linear program.

2. OBJECTIVE FUNCTION

Formulating the search for pathways in reaction networks as an MILP problem, allows us to add an implication constraint to rule out pathways containing one or more individual transitions not favored by thermodynamics. However, it also enables us to exploit another feature of MILPs, namely the objective function to quantify how likely is the entire pathway to occur.

We would like to formulate the search for pathways as an optimization problem aimed at maximizing the outflow of the target molecule(s). To maximize the intended objective, we attempt to maximize the net thermodynamic force driving the flow. Considering the net thermodynamic forces driving the flow to be the sum of the thermodynamic driving force for each individual transition in the pathway, we choose as objective function the minimization of the cumulative sum of the difference in chemical potentials for each constituent transition with a non-zero flow.

$$\max \left(\sum_{e: f_e > 0} x_e^{\Delta G} \right) \quad (8)$$

This choice of the objective function (8) is a heuristic which fits well with the cost of perturbing the system so that queried flow is effected with all transitions being thermodynamically driven in the required directions.

The motivation behind choosing this particular objective function can also be argued for from the perspective of maximizing the probability of the occurrence of the pathway. We interpret the free energy difference to be the measure of the probability of the transition as

$$p(e) \sim \exp(-x_e^{\Delta G}) \quad (9)$$

Assuming individual transitions in the pathway as independent events, the probability that the sequence of transitions in the pathway occurs is given by

$$\begin{aligned} p \left(\bigwedge_{e: f_e > 0} e \right) &= \prod_{e: f_e > 0} p(e) \\ &\sim \prod_{e: f_e > 0} \exp(-x_e^{\Delta G}) \\ &= \exp \left(- \sum_{e: f_e > 0} x_e^{\Delta G} \right) \end{aligned}$$

Since, $\forall(x, y): x \leq y \iff \exp(x) \leq \exp(y)$, maximizing the probability that the pathway is encountered is equivalent to minimizing the objective function (Equation (8)).

3. TEMPORAL ORDERING OF MOLECULES

We note that the ILP formulation of the problem [15] accounts for flow conservation for each molecule, but not for any temporal ordering of the transitions in the returned flow. In special scenarios, such as synthesis planning [19, 20], we would like to interpret a pathway strictly as a directed acyclic process that generates the target molecule(s). We therefore introduce constraints to enforce a temporal order on the found pathways.

The ordering is implemented by introducing a supplementary integer variable t_v for each vertex v which keeps track of their ordering in the pathway. The condition $t_u < t_v$ implies that vertex u is visited by the flow before vertex v . Formally this is ensured by the following implication constraint:

$$\forall e \equiv (e^-, e^+) \in E: f_e > 0 \implies t_u \geq t_v + 1, \forall \text{ pairs } u, v \text{ such that } u \in e^-, v \in e^+ \quad (10)$$

That is, the constraint ensures that reactants are assigned a lower order than products of a transition with flow. We acknowledge that it can be too restrictive to enforce constraints to return pathways with an assigned temporal ordering of vertices because they would eliminate all pathways with cycles in them. Cycles are present whenever catalysts are used and in numerous metabolic networks. We merely suggest the possibility of adding such constraints as a part of the larger MILP model. There might be other use cases where these temporal constraints should be disabled in the model. In these cases, the realizability question for pathways can be addressed using a separate, more robust tool using the computationally more involved formalism Petri nets on top of the MILP solver. We refer the reader to [21] for a more detailed treatment of this issue of realizability of pathways.

B. IMPLEMENTATION

The objective function is a conditional sum for a set of MILP variables. The value of the variable $x_e^{\Delta G}$ contributes to the objective function only if the corresponding hyperedge is used in the pathway. It needs to be converted into a simple linear sum of a set of MILP variables before the MILP solver can evaluate it. Additionally, several constraints in the mathematical formulation of the problem have been specified as implications. Also they need to be linearized before fed into the MILP solver. This section describes these implementation details for the formulated MILP model in Section III A.

1. IMPLEMENTING THE OBJECTIVE FUNCTION

The objective function minimizes the cumulative sum of the differences in chemical potentials along the pathway, $\min \left(\sum_{e: f_e > 0} x_e^{\Delta G} \right)$, rather than the simple sum of differences in chemical potentials. For all transitions e , $\min \left(\sum_{e \in E} x_e^{\Delta G} \right)$, in the reaction network. For each hyperedge e , a binary variable $z_e \in \{0, 1\}$ is introduced, indicating whether that hyperedge is used in the pathway, by the following constraints

$$z_e = 0 \iff f_e = 0 \tag{11}$$

$$z_e = 1 \iff f_e > 0 \tag{12}$$

We define an additional variable $\bar{x}_e^{\Delta G}$ for each hyperedge.

The assignment of the variables $\bar{x}_e^{\Delta G}$ is done by the following constraints

$$\bar{x}_e^{\Delta G} = 0 \iff z_e = 0 \tag{13}$$

$$\bar{x}_e^{\Delta G} = x_e^{\Delta G} \iff z_e = 1 \tag{14}$$

The objective function is defined as the sum of these $|E|$ variables for all hyperedges in the hypergraph; $\min \left(\sum_{e \in E} \bar{x}_e^{\Delta G} \right)$. Hyperedges that are not utilized by the pathway have $\bar{x}_e^{\Delta G} = 0$ and would not contribute to the value of the objective function, implementing the objective function as a linear expression.

2. LINEARIZING THE CONSTRAINTS

The bi-implication constraints, Equations (11) and (12), associating the boolean variable z_e to the edges e is implemented using the big-M method [22], where $M > 0$ is a large positive integer constant²

$$\forall e \in E: \tag{15}$$

$$z_e \leq f_e$$

$$M \cdot z_e \geq f_e \tag{16}$$

The expansion of how the added linear constraints in Equations (15) and (16) lead to assignment of z_e satisfying the implication constraints in Equations (11) and (12) is shown in Table I.

² The constant M has to be larger than the possible values of the variables in the MILP formulation which include the flows f_e for the hyperedges and the chemical potentials $x_v^{G^0}$ for the vertices (in atomic units). In our present implementation $M = 100$ suffices.

Case of f_e	(15)	(16)	Implication for z_e
$f_e = 0$	$z_e \leq 0$	$M \cdot z_e \geq 0$	$z_e = 0$
$f_e = k > 0$	$z_e \leq k$	$M \cdot z_e \geq k$	$z_e = 1$

TABLE I. The linear constraints in Equations (15) and (16) are equivalent to the bi-implication constraints in Equations (11) and (12).

Case of f_e	Implication for z_e	Case of $x_e^{\Delta G}$	(5) satisfied?	(17) satisfied?
$f_e = 0$	$z_e = 0$	$x_e^{\Delta G} > 0$	True	True
$f_e = 0$	$z_e = 0$	$x_e^{\Delta G} \leq 0$	True	True
$f_e > 0$	$z_e = 1$	$x_e^{\Delta G} > 0$	False	False
$f_e > 0$	$z_e = 1$	$x_e^{\Delta G} \leq 0$	True	True

TABLE II. The linear constraint in Equation (17) is equivalent to the implication constraint in Equation (5).

The implication constraint in Equation (5) determines if an hyperedge can be used in the flow depending on the differences in the chemical potentials for the hyperedges $x_e^{\Delta G}$. This is linearized as

$$\forall e \in E: \\ x_e^{\Delta G} + M \cdot (z_e - 1) \leq 0 \quad (17)$$

The equivalence of the added linear constraints in Equation (17) to the implication constraint in Equation (5) is shown in Table II.

The bi-implication constraints in Equations (13) and (14) assigns the variable $\bar{x}_e^{\Delta G}$ with the differences in the chemical potentials for the hyperedges for the evaluation of the objective function. By utilizing the variables z_e , we implement the constraints as

$$\forall e \in E: \\ x_e^{\Delta G} - \bar{x}_e^{\Delta G} \leq M(1 - z_e) \quad (18)$$

$$x_e^{\Delta G} - \bar{x}_e^{\Delta G} \geq -M(1 - z_e) \quad (19)$$

$$\bar{x}_e^{\Delta G} \leq M \cdot z_e \quad (20)$$

$$\bar{x}_e^{\Delta G} \geq -M \cdot z_e \quad (21)$$

The expansion of how the added linear constraints in Equations (18), (19), (20), and (21) lead to desired assignment of $\bar{x}_e^{\Delta G}$ satisfying the implication constraints in Equations (13) and (14) is shown in Table III.

Case of z_e	Case of $x_e^{\Delta G}$	Constraint on $\bar{x}_e^{\Delta G}$ by				Implication for $\bar{x}_e^{\Delta G}$
		(18)	(19)	(20)	(21)	
$z_e = 0$	$x_e^{\Delta G} > 0$			≤ 0	≥ 0	$= 0$
$z_e = 0$	$x_e^{\Delta G} \leq 0$			≤ 0	≥ 0	$= 0$
$z_e = 1$	$x_e^{\Delta G} > 0$	Cannot happen				
$z_e = 1$	$x_e^{\Delta G} \leq 0$	$\geq x_e^{\Delta G}$	$\leq x_e^{\Delta G}$			$= x_e^{\Delta G}$

TABLE III. The linear constraints of Equation (18), (19), (20), and (21) assign $\bar{x}_e^{\Delta G}$ according to the bi-implication constraints in Equations (13) and (14). Note that the third case cannot happen due to Equation (5), because $x_e^{\Delta G} > 0 \implies f_e = 0 \implies z_e = 0$.

The implication constraint in Equation (10) assigns the temporal ordering t_v to each vertex v . It is implemented as a linear constraint as

$$\forall \text{ pairs } u, v \text{ where } \exists e = (e^-, e^+) \text{ such that } u \in e^-, v \in e^+ : \quad (22)$$

$$t_v - t_u - |V|(z_e - 1) - 1 \geq 0$$

$$\forall v \in V, \quad (23)$$

$$0 \leq t_v \leq |V|$$

The constraint in Equation (22) enforces the assignment $t_v > t_u$ only if the corresponding hyperedge is used in the hyperflow. The size of the vertex set for the hypergraph $|V|$ is used in place of the large integer M in the constraint in Equation (22) and as an upper bound for the temporal ordering variable t_v for each vertex v in the constraint in Equation (23). The number of constraints added to the MILP model to determine the topological sorting of the vertices is $\mathcal{O}(|V|^2)$.

C. IMPLEMENTED MODEL

For an overview, we here list the entire set of variables of the model in Table V and the constants used in the model in Table IV. We also summarize the mixed integer linear program developed in Sections III A and III B. This model is what is given to the MILP solver.

$$\min \left(\sum_{e \in E} \bar{x}_e^{\Delta G} \right) \quad (24)$$

$$\forall v \in V: \sum_{e \in \bar{E}} s_{ve}^+ f_e - \sum_{e \in \bar{E}} s_{ve}^- f_e = 0 \quad (2)$$

$$\text{Structural specification constraints on } f_e \text{ for } e \in \bar{E} \quad (3)$$

$$\forall e \equiv (e^-, e^+) \in E:$$

$$0 \leq f_e \quad (4)$$

$$0 \geq x_e^{\Delta G} + M \cdot (z_e - 1) \quad (17)$$

$$x_e^{\Delta G} = \left(\sum_{v \in e^+} x_v^{G^0} - \sum_{v \in e^-} x_v^{G^0} \right) + RT \cdot \left(\sum_{v \in e^+} x_v^K - \sum_{v \in e^-} x_v^K \right) \quad (6)$$

$$M(1 - z_e) \geq x_e^{\Delta G} - \bar{x}_e^{\Delta G} \quad (18)$$

$$-M(1 - z_e) \leq x_e^{\Delta G} - \bar{x}_e^{\Delta G} \quad (19)$$

$$M \cdot z_e \geq \bar{x}_e^{\Delta G} \quad (20)$$

$$-M \cdot z_e \leq \bar{x}_e^{\Delta G} \quad (21)$$

$$\forall (u, v) | u \in e^-, v \in e^+:$$

$$0 \leq t_v - t_u - |V|(z_e - 1) - 1 \quad (15)$$

$$\forall v \in V:$$

$$0 \leq t_v \leq |V| \quad (16)$$

$$[x_v^K]_{\min} \leq x_v^K \leq [x_v^K]_{\max} \quad (7)$$

The computational complexity of finding MILP solutions is in general NP-hard [23], and even the restricted case of finding chemical pathways remains so [24]. Despite this worst case complexity, modern MILP solvers efficiently handle most practically relevant instances in reasonable time. From a thermodynamic perspective, it is often valuable to explore *multiple* optimal or near-optimal solutions—however, MILP solvers generally only provide a single optimal solution. Some solvers, e.g., IBM ILOG CPLEX, do provide a so-called solution pool facility for enumerating multiple solutions, but there is little user-control for how it is populated, and in particular how solutions are compared for equality.

The thermodynamics module described in this contribution is implemented as an extension of the larger software package MØD [13], available at <http://mod.imada.sdu.dk/>. The package offers

Constant	datatype	description
M	integer	a big integer used for linearizing the constraints (type promoted to float, if required)
$x_v^{G^0}$	float	chemical potential of a vertex v under standard physical conditions as assigned by the thermodynamic oracle
$x_e^{\Delta G^0}$	float	differences in chemical potential of in-vertices and out-vertices of a hyperedge e under standard physical conditions

TABLE IV. Constants in the proposed MILP formulation. The constants M and $x_v^{G^0}$ are provided as input, while the constants $x_e^{\Delta G^0}$ are calculated based on the given $x_v^{G^0}$.

MILP variable	datatype	description
f_e	integer	flow variable for a hyperedge e , non-negative
z_e	boolean	indicator variable for a hyperedge e denoting if it is used in the flow
$x_e^{\Delta G}$	float	differences in chemical potential of in-vertices and out-vertices of a hyperedge e after accounting for their concentrations
$\bar{x}_e^{\Delta G}$	float	copy of $x_e^{\Delta G}$ used in the (linearized) objective function
x_v^K	float	log concentration of a vertex v
t_v	integer	topological ordering number for vertex v , non-negative

TABLE V. Variables in the proposed MILP formulation.

the option of using multiple MILP solvers, currently IBM ILOG CPLEX, Gurobi, and Coin-OR CBC. For the results presented here we have used Coin-OR CBC [25]. MØD implements a MILP enumeration algorithm on top of the solver in use, where one can specify a set of integer og binary variables to enumerate over. This enumeration in MØD proceeds as tree search algorithm over the domains of this set of variables, with calls to the MILP solver for evaluating feasibility obtaining optimal solutions of subproblems [15].

In the MILP model presented here, there are variables with a continuous domain representing the concentrations and chemical potentials of the molecules. We do not consider minor changes in these variables to represent a new solution, as long as the underlying flow is unchanged. Hence, we carry out the enumeration over the variables $f_e, \forall e \in E$. The resulting output is a list of different integral flows, listed in the order of increasing value of the objective function (Equation (24)).

D. THERMODYNAMIC ORACLE

Given a reaction network, we assign chemical potentials to the molecules using what we had earlier referred to as a ‘thermodynamic oracle’. Utilizing quantum mechanical methods based on DFT as this ‘thermodynamic oracle’ quickly becomes impractical as the number of electrons in the molecule (denoted by n) increases. Calculating the electron density in a molecule using DFT is an iterative process. Each step invokes gradient descent, which scales beyond $\mathcal{O}(n^3)$ for classical DFT based methods for a single-point calculation because it involves matrix inversions. After the electron density for the molecule has been optimized, it can then be used to calculate the electronic contribution to the energy of a molecule. Although machine learning methods exist for potential assignment, they still require optimized atomic coordinates to determine potentials [26]. Ideally, kinetic rate parameters would have to be incorporated into the search for pathways in a reaction network as integer flows, because they dictate which transitions actually occur in the system and how fast. However, calculating activation free energies using DFT-based quantum mechanical methods to determine these kinetic parameters would demand even further time and computational resources.

As an alternative, we in this work adopt a compromise oracle based on equilibrium thermodynamics. This approximation has some theoretical basis behind it with the Evans–Polanyi–Semenov principle, which states that within a class of transitions, the thermodynamics of the transition acts as a proxy for the kinetics of the transition. It allows us to substitute the energy barrier for a transition with the free energy difference for a transition resulting in the relation in Equation (9). Specifically, to balance accuracy, efficiency, generalizability, and running time, we employ a semi-empirical method, GFN2-xTB [17], for potential assignment. While this method compromises on accuracy compared to DFT, the errors are acceptable for demonstrating the utility of the mathematical model on an example reaction network. We detail the thermodynamic oracle we use to assign the chemical potentials to the molecules in the reaction network in Appendix A 1. An advantage of this modular approach is that it provides the reader the freedom to substitute the proposed thermodynamic oracle with another tool mapping a molecule to its chemical potential depending on the desired accuracies and available computational resources.

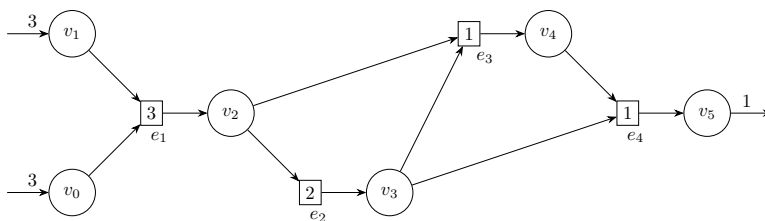
IV. RESULTS

In this section, we demonstrate the methods from Section III on a reaction network involving hydrogen cyanide, formamidic acid, and formamide in aqueous solution which has been studied in

[27]. The reaction network was generated using MØD by the expansion of the molecular space with the seed molecules HCN , NH_3 , and H_2O , by the recursive application of the graph transformation rules listed in Appendix A 3. In the graphs in Appendix A 3, individual molecules are represented as undirected labeled graphs (with the atoms represented as vertices, labeled by the symbols of the elements and the bonds are represented as edges, labeled by bond types). Stereo-information is not represented. Molecular graphs also constitute the vertices of the hypergraph representing the reaction network. The graph transformation rules in Appendix A 3 represent classes of reactions, i.e. reaction templates. The left hand side of the rules is a subgraph, which may be substituted by the subgraph on the right hand side, when a match has been found in a molecular graphs present in the reaction network. This executes a reaction, thereby expanding the molecular space. Following the previous study of the network [27], the expansion was constrained to only generate molecules with a maximum of three carbon, three nitrogen, and three oxygen atoms. Moreover, only stable molecules ($x_v^{G^0} \leq 0$) were kept. The generated reaction network consists of 67 vertices and 202 hyperedges, and is shown in Figure 9 for completeness. A list of all molecules and transitions in the reaction network can be found in the associated GitHub repository [28]. An estimate for the atomic coordinates for the molecules was deduced from their connectivity using Open Babel [29]. Using xTB [17], this geometry was then refined and used to calculate the chemical potentials under standard conditions with water as the solvent.

The primary objective was to study the energetics of condensation pathways of the smaller seed molecules (HCN , NH_3 , and H_2O) into larger oligomers, which might have implication for the pre-biotic synthesis of amino acids and compare it with the pathways reported in [27]. Therefore, the formulated MILP model was set up to query the pathways with HCN , NH_3 , and H_2O as the input molecules and the trimer of formamide (numbered 17 in [27]) as the target molecule. The formulated MILP to search for pathways with the given input and output vertices had 336 variables. As a sanity check, the enumerated list of flow solutions returned by the solver included the pathway suggested in [27], thought not as the optimal solution when scored according to Equation (24). This is depicted in Figure 3. The sum of free energies of the transitions in this pathway is $-178.412 \text{ kJ mol}^{-1}$, while the sum of free energies weighted by the number of times it is used in the pathway yields $-405.332 \text{ kJ mol}^{-1}$. This pathway uses four unique transitions (hyperedges). Two of them are used multiple times, which makes seven transitions in total (sum of flows assigned to the hyperedges).

While thermodynamics might provide an insight to the equilibrium flows in the reaction network, it does not describe the path to that equilibrium. Each transition has an associated barrier energy that must be overcome for the transition to occur. Enumerating pathways using our implementation of the

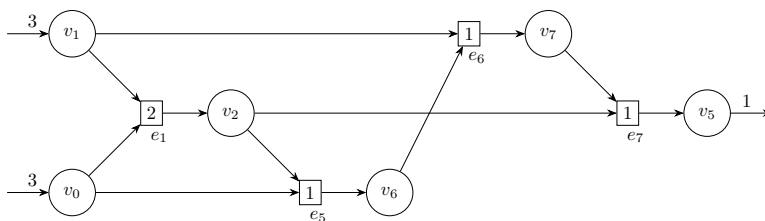


vertex	molecular structure	in [27]
v_0	HCN	1
v_1	H ₂ O	not numbered
v_2	<chem>HO-C(=O)-NH</chem>	4
v_3	<chem>O=C-NH2</chem>	5
v_4	<chem>O=C-N(O)-NH2</chem>	16
v_5	<chem>O=C-N(O)-N(O)-NH2</chem>	17

vertex	inFlow	outFlow	$x_v^{\Delta G}$	x_v^K	t_v	hyperedge	f_e	in(v)	out(v)	$\bar{x}_e^{\Delta G}$
v_0	3	0	-5.507	1.000	0	e_1	3	v_0, v_1	v_2	-94.141
v_1	3	0	-5.068	-6.000	0	e_2	2	v_2	v_3	-38.629
v_2	0	0	-10.610	-6.000	1	e_3	1	v_2, v_3	v_4	-0.006
v_3	0	0	-10.625	0.195	2	e_4	1	v_3, v_4	v_5	-45.645
v_4	0	0	-21.249	-1.190	5	$\sum_e \bar{x}_e^{\Delta G} = -178.412$				
v_5	0	1	-31.869	-6.000	8	$\sum_e f_e \cdot \bar{x}_e^{\Delta G} = -405.332$				

FIG. 3. (Top) The pathway with the sum of free energies $-178.412 \text{ kJ mol}^{-1}$ and (center) the molecules used with the corresponding number in [27]. (Bottom) The MILP solution: the $x_v^{\Delta G}$ values are in atomic units (from xTB) while the $\bar{x}_e^{\Delta G}$ are in kJ mol^{-1} . The x_v^K values are the dimensionless equivalent of $\log_{10} \frac{[\text{concentration}]}{1 \text{ mol lit}^{-1}}$.

MILP formulation of the problem provides the pathway in Figure 4 as one with the minimum value of the objective function. This pathway utilizes four unique transitions and five transitions in all to realize the pathway, which is fewer than the previously reported pathway. Since the difference in the chemical potential between the source and target molecules is fixed, choosing hyperedges with larger free energy differences would increase the value of the objective function. Using transition with larger



vertex	molecular structure	in [27]
v_0	HCN	1
v_1	H ₂ O	not numbered
v_2	<chem>HO-C#N</chem>	4
v_6	<chem>HO-C#N-C#N</chem>	not present
v_7	<chem>HO-C#N-C(O)N</chem>	tautomer of 16
v_5	<chem>O=C(N)C(O)C(O)N</chem>	17

vertex	inFlow	outFlow	$x_v^{\Delta G}$	x_v^K	t_v	hyperedge f_e	in(v)	out(v)	$\bar{x}_e^{\Delta G}$	
v_0	3	0	-5.507	1.000	0	e_1	2	v_0, v_1	v_2	-94.141
v_1	3	0	-5.068	-6.000	0	e_5	1	v_0, v_2	v_6	-129.554
v_2	0	0	-10.610	1.000	1	e_6	1	v_1, v_6	v_7	-38.298
v_6	0	0	-16.159	-6.000	2	e_7	1	v_2, v_7	v_5	-51.185
v_7	0	0	-21.240	1.000	3	$\sum_e \bar{x}_e^{\Delta G} = -313.178$				
v_5	0	1	-31.869	-6.000	5	$\sum_e f_e \cdot \bar{x}_e^{\Delta G} = -407.319$				

FIG. 4. (Top) The pathway with minimum sum of free energies ($-313.178 \text{ kJ mol}^{-1}$) returned as the optimal by our model and (center) the molecules used with the corresponding number in [27]. (Bottom) MILP solution for the optimal pathway: the $x_v^{\Delta G}$ values are in atomic units (from xTB) while the $\bar{x}_e^{\Delta G}$ are in kJ mol^{-1} . The x_v^K values are the dimensionless equivalent of $\log_{10} \frac{[\text{concentration}]}{1 \text{ mol lit}^{-1}}$.

free energy differences to ‘cover’ the net difference in the chemical potential, lead to fewer transitions being used in the pathway.

The main source of difference in the objective function value in the two pathways is the chemical

potential of the molecule v_6 that is not present in the conventional pathway. While the conventional pathway in [27] is more symmetric and appealing because of the stepwise nucleophilic attack on the carbonyl C atom by the amine N atom of an adjacent v_3 molecule, which is repeated twice to generate v_5 , [27] also notes that these condensation reactions have a positive Gibbs free energy. To quote the authors, ‘each step is endergonic although decreasingly so. Dimerization of formamide is uphill 19.8 kcal/mol, owing to the thermodynamic stability of the monomers in solution. Addition of another monomer to form the trimer, via similar nucleophilic attack, is uphill 19.0 kcal/mol’. This can also be observed in the ILP solution in bottom-right Table 3 for the conventional pathway where the hyperedges $e_3 \equiv (\{v_2, v_3\}, \{v_4\})$ have a $\bar{x}_e^{\Delta G}$ value close to zero. The constraint in Equation (5) forces the hyperedge to have $\bar{x}_e^{\Delta G} \leq 0$ for it to be included in the pathway. The MILP solver chooses the log concentration variables x_v^K for the molecules v_3 and v_4 in such a way so that $\bar{x}_e^{\Delta G}$ variables for e_3 is just below zero to realize the pathway. This might be the reason for x_v^K for these two vertices not having the extremal value as is often the case, as discussed below. Our proposed model also returns an alternative pathway involving v_6 , where none of the $\bar{x}_e^{\Delta G}$ weights for the hyperedges is close to zero.

We observe that the log concentration variables are always assigned extremal values decided by the constraint in Equation (7). This is likely an artifact of using an MILP solver with an objective function for the problem. An MILP is a convex optimization problem where minimizing the objective function (involving a subset of the MILP variables) results in a solution located at a vertex of the convex space defined by the constraints. The bounds for the variables are hand-crafted by the user and it might be more realistic to assign different bounds for the log concentration variable for each vertex. Alternatively, a better interpretation of the assigned values for the variables, x_v^K might be the direction in which the equilibrium concentrations have to be perturbed to achieve the desired flow. For example, the concentration values in bottom-left Table of Figure (4) can be interpreted as the concentrations of v_1 , v_6 and v_5 have to be lowered and the concentrations of v_0 , v_2 and v_7 have to be raised to achieve a larger difference in the potentials while effecting a net outflow of molecule v_5 given input molecules v_0 and v_1 .

An exhaustive search of the reaction space led to the identification of several reaction pathways with interesting features, as depicted in the appendix. The next-best feasible solutions are tabulated in Table VI.

V. DISCUSSION

In this section, we give a detailed comparison of our methods with some existing frameworks. One of the closest is *thermodynamics-based metabolic flux analysis* (TMFA) [2] which also utilizes mixed

$\sum_e z_e$	$\sum_e f_e$	#vertices	$\sum_e z_e \cdot x_e^{\Delta G}$	$\sum_e f_e \cdot x_e^{\Delta G}$
6	7	8	-313.178 (0)	-407.319
4	5	6	-313.178 (1)	-407.319
5	6	7	-313.178 (2)	-407.319
5	6	7	-313.178 (3)	-407.319
5	7	7	-243.966 (4)	-406.204
4	6	6	-243.966 (5)	-406.204
3	5	5	-243.966 (6)	-406.204
5	7	7	-243.966 (7)	-406.204
3	5	5	-243.966 (8)	-406.204
4	6	6	-243.966 (9)	-406.204
4	6	6	-243.966 (10)	-406.204
4	6	6	-243.966 (11)	-406.204
4	6	6	-243.966 (12)	-406.204
5	7	7	-243.966 (13)	-406.204
4	7	6	-178.412 (14)	-405.332
5	8	7	-178.412 (15)	-405.332
4	7	6	-178.412 (16)	-405.332
4	7	6	-178.412 (17)	-405.332

TABLE VI. Pathways to the formation of the target molecule.

integer linear constraints. Despite similarities in parts of the thermodynamic modeling, the problem solved is different, with some of the key differences being:

- TMFA generates *flux distributions* not containing thermodynamically infeasible reactions, while our method searches for *explicitly specified pathways* not containing thermodynamically unfavorable reactions. The flux vector generated by TMFA is real-valued as opposed to integer values for the flows in the pathways determined by our method. In many settings, the concept of a pathway involves an integer number of molecules participating in each reaction of the pathway, which aligns well with integer flows.
- TMFA uses a curated dataset of metabolites with chemical potentials determined by group contribution methods. In our case a semi-empirical method (GFN2-xTB) is used to assign chemical potentials to the molecules in the reaction network. However, it can be substituted by any suit-

able ‘oracle’ that maps a molecule to its Gibbs free energy of the user choice. This provides flexibility and a wider applicability to this method.

- We allow for a ranking of the enumerated results based on thermodynamics-based metrics. In terms of the linear program modeling, restricting the flow variables to integers allows us to enumerate solutions over the integral variables (i.e., to generate not just a single solution, but many). Additionally, we can enforce a partial ordering of the vertices in the returned integer hyperflow solutions, in order to guarantee their realizability as synthesis plans.

We now turn to a comparison with some of the other existing frameworks. Formulating the problem as an MILP allows us to leverage the many algorithmic advances made in the field of MILP solvers. This may be one reason why we are able to analyze larger reaction networks than those analyzed in [3, 30, 31] involving a smaller number of distinct molecules. A further difference to these works is that they utilize kinetic rate equations derived from the law of mass action (reactions under kinetic control), while our focus is on the differences in chemical potentials of the molecules in the reaction network near equilibrium (reactions under thermodynamics control).

Weighted directed graphs are utilized in [1] to model the thermodynamic phase space of a reaction network. However, instead of a constant positive edge weight derived from the Gibbs free energy of the reaction, we utilize the free energies themselves to allow for an analysis more directly based on thermodynamics. Several other cheminformatics tools and automated protocols for computationally exploring reaction networks utilize reactive molecular dynamics simulations [32–34] or chemical heuristics [35–38]. However, to the best of our knowledge, there does not exist any computational framework for explicitly specifying and searching for pathways in reaction networks while simultaneously incorporating thermodynamic constraints in the present form.

VI. CONCLUSION

Thermodynamics emerged from efforts to analyze the operation of steam engines while maximizing the work done by them. In a nice analogy, the search for pathways may be phrased as viewing reaction networks as chemical engines in which we want to maximize the output of some target molecule(s). Recognizing that thermodynamics, encapsulated by the Gibbs free energies of the transitions, play a pivotal role in determining the probability of a transition occurring, we in this paper have focused on developing new ways to integrated thermodynamics into the search for pathways.

Exploring pathways with favorable energy profiles involves a challenging navigation of a large and complex energy landscape where the driving thermodynamic forces are influenced by the concentra-

tion ratios, inflows of the source molecules and outflows of the target molecules. This work is an attempt at addressing part of that challenge. However, there might be several refinements possible, some of which we list here:

1. The constraint enforcing that only transitions with negative free energies are allowed in the returned pathways (implemented through the constraint in Equation (5)) might be overly stringent. Under experimental conditions, the reactions observed to occur do not always align with those predicted to occur theoretically. Transitions, such as the thermal decomposition of lithium carbonate are observed to occur in practice despite being predicted to be thermodynamically unfavorable using computed (or experimental) free energies for the transition. On the other hand, transitions predicted to be thermodynamically favorable do not always occur in practice because they have a high energy barrier (like the allotropic conversion of diamond into graphite). Therefore, there should be some flexibility in delineating the boundary between those transitions are considered likely and included in the pathway and those that are not to bring the model closer to reality. Such extensions of the current modeling should be fairly straightforward.
2. The objective function used minimizes the sum of Gibbs free energies of the transitions in the pathway. However, this approach might favor a pathway with more extreme values for the free energies rather than one with more moderate free energies. Therefore, it might be worthwhile to explore alternative objective functions too, such as the min-max besides the min-sum used currently.
3. The current formulation completely disregards the kinetics of individual transitions. However, the probability of a transition occurring is determined to a substantial extent by the reaction barrier height, and not only by the concentration of the reactants and the products. As a result, our framework might include a transition in the returned pathway with a favorable thermodynamic driving force, but too high an reaction barrier, making it a slow and rate-limiting step for the entire pathway. On the other hand, coming up with a generic ‘kinetic oracle’ with a wide applicability to estimate the barrier heights for diverse transitions poses a significant challenge. The transition states determining the barrier heights are saddle points on the potential energy surface, unlike the reactants and products that are minima and can be located by gradient descent optimization methods.

Hence, we do not claim our work to be the final word in the quest for incorporating thermodynamics into the search for pathways in reaction networks. Still, we believe that it constitutes a valuable

step forward, and we end by summarizing its virtues: We provide a systematic and thermodynamically informed approach to optimize the computational search for pathways in reaction networks.

Modeling pathways as integer hyperflows gives results that can be interpreted in mechanistic terms, as each molecule is present in integral quantities. Formulating the problem as an MILP problem and utilizing an MILP solver allows us to obtain solutions with reasonable computational resources and time. It also enables enumeration of pathways over the integral flow variables, facilitating a systematic exploration of pathways in the reaction network. Returning several solutions to pathway queries is an asset, as the answer becomes more robust to the possible errors in the calculations of chemical potentials of the molecules and to other artifacts of the simplification of reality inherent in any modeling. Moreover, it offers alternatives to choose from if the optimal solution turns out to be unattainable under controlled industrial reactor or laboratory conditions.

Finally, the application in Section IV of our framework to a reaction network based on a real-life chemistry acts as a proof-of-concept and illustrates the computational feasibility and analytic potential of our methods.

ACKNOWLEDGMENTS

This work was supported by generous funding from the European Union’s Horizon 2021 Research and Innovation program under Marie Skłodowska-Curie grant agreement no. 101072930 (TACsy — Training Alliance for Computational systems chemistry) and also by the European Union and the Swiss State Secretariat for Education, Research and Innovation (SERI) under contract numbers 22.00017 and 22.00034 (Horizon Europe Research and Innovation Project CORENET). In addition, the authors would like to thank Dr. Maike Bergeler, Digitalization of R&D - Quantum Chemistry at BASF, Ludwigshafen am Rhein, Germany for her assistance and inputs regarding the use of the xTB software.

REFERENCES

-
- [1] M. J. McDermott, S. S. Dwaraknath, and K. A. Persson, A graph-based network for predicting chemical reaction pathways in solid-state materials synthesis., Nat Commun **12**, [10.1038/s41467-021-23339-x](https://doi.org/10.1038/s41467-021-23339-x) (2021).

- [2] C. S. Henry, L. J. Broadbelt, and V. Hatzimanikatis, Thermodynamics-based metabolic flux analysis, *Bio-physical Journal* **92**, 1792 (2007).
- [3] T. Schmiedl and U. Seifert, Stochastic thermodynamics of chemical reaction networks, *The Journal of Chemical Physics* **126**, 044101 (2007).
- [4] R. Rao and M. Esposito, Nonequilibrium thermodynamics of chemical reaction networks: Wisdom from stochastic thermodynamics, *Phys. Rev. X* **6**, 041064 (2016).
- [5] F. Avanzini, N. Freitas, and M. Esposito, Circuit theory for chemical reaction networks, *Phys. Rev. X* **13**, 021041 (2023).
- [6] G. Szederkényi and K. Hangos, Finding complex balanced and detailed balanced realizations of chemical reaction networks., *J Math Chem* **49**, 1163–1179 (2011).
- [7] G. Szederkényi and K. Hangos, Finding complex balanced and detailed balanced realizations of chemical reaction networks., *J Math Chem* **49**, 1163–1179 (2011).
- [8] M. Johnston, D. Siegel, and G. Szederkényi, A linear programming approach to weak reversibility and linear conjugacy of chemical reaction networks., *J Math Chem* **50**, 274–288 (2011).
- [9] M. Johnston, Analysis of mass-action systems by split network translation., *J Math Chem* **60**, 195–218 (2021).
- [10] M. J. Willis and M. von Stosch, Inference of chemical reaction networks using mixed integer linear programming, *Computers & Chemical Engineering* **90**, 31 (2016).
- [11] J. L. Andersen, MØD, <http://mod.imada.sdu.dk> (2024).
- [12] J. L. Andersen, C. Flamm, D. Merkle, and P. F. Stadler, An intermediate level of abstraction for computational systems chemistry, *Philosophical Transactions of the Royal Society A: Mathematical, Physical and Engineering Sciences* **375**, 20160354 (2017).
- [13] J. L. Andersen, C. Flamm, D. Merkle, and P. F. Stadler, A software package for chemically inspired graph transformation, in *Graph Transformation*, edited by R. Echahed and M. Minas (Springer International Publishing, Cham, 2016) pp. 73–88.
- [14] J. L. Andersen, C. Flamm, D. Merkle, and P. F. Stadler, Generic strategies for chemical space exploration, *IJCBDD* **7**, 10.1504/IJCBDD.2014.061649 (2014).
- [15] J. L. Andersen, C. Flamm, D. Merkle, and P. F. Stadler, Chemical transformation motifs—modelling pathways as integer hyperflows, *IEEE/ACM Transactions on Computational Biology and Bioinformatics* **16**, 510 (2019).
- [16] J. L. Andersen, C. Flamm, D. Merkle, and P. F. Stadler, Defining autocatalysis in chemical reaction networks, *Journal of Systems Chemistry* **8**, 121 (2020), tR: <https://arxiv.org/abs/2107.03086>.
- [17] C. Bannwarth, E. Caldeweyher, S. Ehlert, A. Hansen, P. Pracht, J. Seibert, S. Spicher, and S. Grimme,

- Extended tight-binding quantum chemistry methods, *WIREs Computational Molecular Science* **11**, e1493 (2021).
- [18] S. Müller, C. Flamm, and P. F. Stadler, What makes a reaction network “chemical”?, *J Cheminform* **14**, 10.1186/s13321-022-00621-8 (2022).
- [19] J. Bradshaw, B. Paige, M. J. Kusner, M. H. S. Segler, and J. M. Hernández-Lobato, *Barking up the right tree: an approach to search over molecule synthesis dags* (2020), arXiv:2012.11522 [cs.LG].
- [20] R. Fagerberg, C. Flamm, R. Kianian, D. Merkle, and P. F. Stadler, Finding the k best synthesis plans., *J Cheminform* **10**, 10.1186/s13321-018-0273-z (2018).
- [21] J. L. Andersen, S. Banke, R. Fagerberg, C. Flamm, D. Merkle, and P. F. Stadler, On the realisability of chemical pathways (2023), arXiv:2309.10629 [q-bio.MN].
- [22] M. Cococcioni and L. Fiaschi, The big-m method with the numerical infinite m, *M. Optim Lett* **15**, 2455 (2020).
- [23] R. M. Karp, Reducibility among combinatorial problems, in *Complexity of Computer Computations*, edited by R. E. Miller and J. W. Thatcher (Plenum Press, NY, 1972) pp. 85–103.
- [24] J. Andersen, C. Flamm, D. Merkle, and P. F. Stadler, Maximizing output and recognizing autocatalysis in chemical reaction networks is NP-complete, *J Syst Chem* **3**, 10.1186/1759-2208-3-1 (2012).
- [25] J. Forrest, T. Ralphs, S. Vigerske, H. G. Santos, J. Forrest, L. Hafer, B. Kristjansson, jpfasano, EdwinStraver, M. Lubin, Jan-Willem, rlougee, jpngoncal1, S. Brito, h-i gassmann, Cristina, M. Saltzman, tostrost, B. Pitrus, F. Matsushima, and to st, *coin-or/cbc: Release releases/2.10.11* (2023).
- [26] R. Zubatyuk, J. S. Smith, B. T. Nebgen, S. Tretiak, and O. Isayev, Teaching a neural network to attach and detach electrons from molecules., *Nat Commun* **12**, 10.1038/s41467-021-24904-0 (2021).
- [27] J. Kua and K. L. Thrush, Hcn, formamidic acid, and formamide in aqueous solution: A free-energy map, *The Journal of Physical Chemistry B* **120**, 8175 (2016), PMID: 27016454.
- [28] supplementary data repository on github, <https://github.com/AdittyPal/thermodynamicsWithILP.git> (2024).
- [29] N. Yoshikawa and G. Hutchison, Fast, efficient fragment-based coordinate generation for open babel., *J Cheminform* **11**, 10.1186/s13321-019-0372-5 (2019).
- [30] A. Miangolarra and M. Castellana, On non-ideal chemical-reaction networks and phase separation., *J Stat Phys* **190**, 10.1007/s10955-022-03037-8 (2023).
- [31] A. G. Cantú and G. Nicolis, Toward a thermodynamic characterization of chemical reaction networks, *Journal of Non-Equilibrium Thermodynamics* **31**, 23 (2006).
- [32] E. Martínez-Núñez, G. L. Barnes, D. R. Glowacki, S. Kopec, D. Peláez, A. Rodríguez, R. Rodríguez-Fernández, R. J. Shannon, J. J. P. Stewart, P. G. Tahoces, and S. A. Vazquez, *Automekin2021: An open-*

- source program for automated reaction discovery, *Journal of Computational Chemistry* **42**, 2036 (2021).
- [33] R. J. Shannon, E. Martínez-Núñez, D. V. Shalashilin, and D. R. Glowacki, Chemdyme: Kinetically steered, automated mechanism generation through combined molecular dynamics and master equation calculations, *Journal of Chemical Theory and Computation* **17**, 4901 (2021), pMID: 34283599.
- [34] M. Döntgen, M.-D. Przybylski-Freund, L. C. Kröger, W. A. Kopp, A. E. Ismail, and K. Leonhard, Automated discovery of reaction pathways, rate constants, and transition states using reactive molecular dynamics simulations, *Journal of Chemical Theory and Computation* **11**, 2517 (2015), pMID: 26575551.
- [35] M. Liu, A. Grinberg Dana, M. S. Johnson, M. J. Goldman, A. Jocher, A. M. Payne, C. A. Grambow, K. Han, N. W. Yee, E. J. Mazeau, K. Blondal, R. H. West, C. F. Goldsmith, and W. H. Green, Reaction mechanism generator v3.0: Advances in automatic mechanism generation, *Journal of Chemical Information and Modeling* **61**, 2686 (2021), pMID: 34048230.
- [36] A. G. Dana, M. S. Johnson, J. W. Allen, S. Sharma, S. Raman, M. Liu, C. W. Gao, C. A. Grambow, M. J. Goldman, D. S. Ranasinghe, R. J. Gillis, A. M. Payne, Y.-P. Li, X. Dong, K. A. Spiekermann, H. Wu, E. E. Dames, Z. J. Buras, N. M. Vandewiele, N. W. Yee, S. S. Merchant, B. Buesser, C. A. Class, F. Goldsmith, R. H. West, and W. H. Green, Automated reaction kinetics and network exploration (arkane): A statistical mechanics, thermodynamics, transition state theory, and master equation software, *International Journal of Chemical Kinetics* **55**, 300 (2023).
- [37] T. A. Young, J. J. Silcock, A. J. Sterling, and F. Duarte, autode: Automated calculation of reaction energy profiles— application to organic and organometallic reactions, *Angewandte Chemie International Edition* **60**, 4266 (2021).
- [38] K. M. Shebek, J. Strutz, L. J. Broadbelt, and K. E. J. Tyo, Pickaxe: a python library for the prediction of novel metabolic reactions., *BMC Bioinformatics* **24**, 10.1186/s12859-023-05149-8 (2023).
- [39] P. Salvy, G. Fengos, M. Ataman, T. Pathier, K. C. Soh, and V. Hatzimanikatis, pyTFA and matTFA: a Python package and a Matlab toolbox for Thermodynamics-based Flux Analysis, *Bioinformatics* **35**, 167 (2018).
- [40] Open babel github repository, <https://github.com/openbabel/openbabel> (2024).
- [41] A. K. Rappe, C. J. Casewit, K. S. Colwell, W. A. I. Goddard, and W. M. Skiff, Uff, a full periodic table force field for molecular mechanics and molecular dynamics simulations, *Journal of the American Chemical Society* **114**, 10024 (1992), <https://doi.org/10.1021/ja00051a040>.

A. APPENDICES

1. ON ASSIGNING THE CHEMICAL POTENTIALS

One of the main enhancements to the thermodynamic modeling of reaction networks in this work is a more robust, transparent and generic method of assigning the chemical potentials under standard physical conditions for molecules, $x_v^{G^0}$, compared to relying on thermodynamic databases such as (<https://pytfa.readthedocs.io/en/latest/thermoDB.html>) using the group contribution method, to infer the free energy change for transitions, $x_e^{G^0}$, as done in [39]. Using quantum chemical methods to assign these chemical potentials quickly becomes computationally resource-intensive because the time complexity scales as $\mathcal{O}(N^3)$. The density-functional theory (DFT) calculations involve diagonalization of the $N \times N$ Hamiltonian matrix. The memory requirement scales as $\mathcal{O}(N^2)$ because of the number of two-electron integrals contributing to the energy of the system. Moreover, it is an iterative process which is repeated until an acceptable convergence criteria is reached.

Efficient software design necessitates striking a balance among the components in this work: expanding the molecular space, assigning chemical potentials to the molecules in the space and solving the formulated MILP for queried pathways in the network. If DFT calculations are employed, the calculation of chemical potentials required a significantly longer time compared to the remaining two components. Alternative semi-empirical methods offered a faster yet reasonable accurate way to assign chemical potentials to molecules. Therefore, we utilized xTB [17] to estimate the chemical potentials for the molecules in the expanded reaction network. In the rest of this Section, we describe how we estimate the chemical potentials for the molecules from their representations as graphs.

The molecules in the expanded reaction network were modeled as graphs where individual vertices represented atoms (labeled by the symbol of the corresponding element), while edges represented bonds. The adjacency matrix of this graph was utilized to determine the connectivity for that molecule. Given a connectivity matrix that satisfies the valences of each atom in the molecule, a three-dimensional embedding for the molecule was generated using the VSEPR theory. The `OBBuilder` class from the Open Babel [29, 40] library was employed to generate the three dimensional coordinates for the atoms utilizing a combination of VSEPR rules and commonly encountered fragments.

The generated geometry of the molecule was refined using 1000 iterations of conjugate gradient descent or until the change in energy (in atomic units, calculated using the universal force field [41]) between successive iterations is less than 10^{-4} . Next, the `OBForceField::WeightedRotorSearch()` was utilized to systematically perform a tree-search for a conformer of the molecule with a low energy,

by biasing the expansion of the search tree towards the current low energy conformer. At each iterative expansion step, 25 conformers were generated, and 100 steps of conjugate descent are executed on each. This lead to the generation of conformers with successively lower energies over subsequent iterations. The conformer with the lowest energy identified at the end of this search process was further subjected to 250 iterations of conjugate descent or until the energy tolerance of 10^{-5} is reached. The energy for a conformer at each step was estimated using the universal force field [41]. The result of this search process, the configuration of the low-energy conformer, containing the three dimensional Cartesian coordinate of each atom in the molecule was written into an `.xyz` file.

The `.xyz` coordinate file generated by OpenBabel serves as an input file for xTB. A geometry optimization of the structure is performed with xTB, employing an energy tolerance of 5×10^{-8} Eh and a gradient tolerance of 5×10^{-5} Eh bohr⁻¹. This is followed by the calculation of the Hessian matrix for the optimized structure, and the chemical potentials at 298.15 K using standard translational, rotational, vibrational, and electronic partition functions from statistical mechanics under the coupled rigid-rotor and harmonic-oscillator approximations.

2. ON THE RANGE OF THE CONCENTRATION VARIABLE

Apart from the free energies for the molecules, $x_v^{G^0}$, assigned by the thermodynamic oracle the limits on the log concentration values of the molecules, $[x_v^K]_{\min}$ and $[x_v^K]_{\max}$ have to be assigned by the user. We provide some comments on the choice of these limits in this work. The upper limit for the concentrations is a physical limit bounded by the concentration of the pure substance. Concentration is expressed in the units of moles per liter (mol L⁻¹) for liquids and solutions while in terms of partial pressures (in Pa) for gases. For liquids, the maximum possible concentration value of the reactant would be that of the pure liquid, which is physically constrained by

$$\begin{aligned} 1 \text{ mol of pure liquid} &\equiv M \text{ kg of pure liquid} \\ 1 \text{ mol of pure liquid} &\equiv \frac{M}{\rho} \text{ L of pure liquid} \\ \text{Maximum concentration} &\equiv \frac{\rho}{M} \text{ mol L}^{-1} \end{aligned}$$

For gases, the maximum concentration is imposed by the physical constraint that it has to remain (an ideal) gas following the equation of state $PV = nRT$ so that the equations from the kinetic theory of gasses might still be applied to it. The concentration of a gas under some given physical condition of pressure P and temperature T is

$$\frac{n}{V} = \frac{P}{RT}$$

As the pressure is increased, or the temperature is decreased to increase the concentration, the gas ceases to behave as an ideal gas and starts exhibiting properties of the vapor phase. A change in the physical state of the substance would have a free energy of phase transition involved, and it can no longer be modeled only using the equations considered in Section III C.

The lower limit of the reactants is imposed by practical constraints because there are limits to the dilution that can be achieved under laboratory conditions. For a solution, infinite dilution would lead to no solute (reactant) being present, and hence the transition would not occur. For gases, there are lower limits to pressures that can be achieved in laboratory vacuum settings. Reactions occurring in the solid phase (or on surfaces) are governed by different physical equations and cannot be expressed by this framework. For all practical purposes, we can assume our reactants to be solutions or gases satisfying the condition of a well-stirred reactor.

For this work, we have chosen the limits in the concentration variables as $[x_v^K]_{\min} = -6$ and $[x_v^K]_{\max} = 1$. These correspond to physical values of the concentrations between 10^{-6} mol lit⁻¹ and 10^1 mol lit⁻¹. While micromolar concentrations can be achieved under laboratory conditions using standard fluidics procedures, a concentration of tens of molar is often encountered for pure liquids (the concentration of pure water is 55.56 mol lit⁻¹). While we use the same range for the log concentration values for all the molecules in the reaction network, the user might choose to assign different ranges for different molecules to make the model more realistic.

3. GRAPH TRANSFORMATION RULES USED

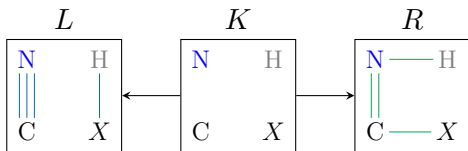


FIG. 5. Rule 1: Addition of water or ammonia to hydrogen cyanide (nitrile group) where $X \in \{N, O\}$ to form an imine. The reverse of this rule was *not* used while expanding the hypergraph.

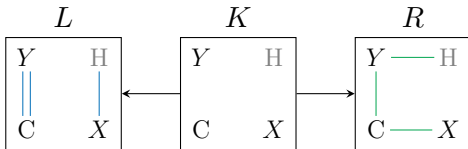


FIG. 6. Rule 2: Addition of water or ammonia to a double bond where $X, Y \in \{N, O\}$ (in an imine or carbonyl group respectively). The reverse of this rule was also used while expanding the hypergraph.

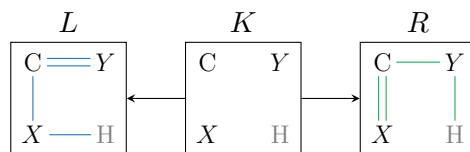


FIG. 7. Rule 3: 1,2 to 2,3 bond shift of the double bond to form tautomers where $X, Y \in \{N, O\}$. The reverse of this rule was also used while expanding the hypergraph.

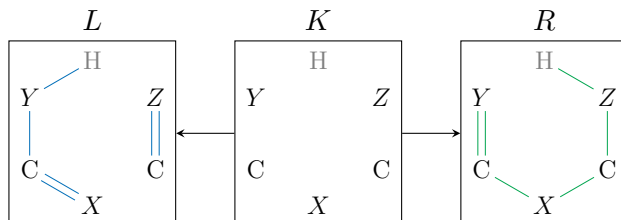


FIG. 8. Rule 4: Addition of two molecules involving six atoms, where $X, Y, Z \in \{N, O\}$, modeling an aldol like addition to carbonyls and imines. The reverse of this rule was also used while expanding the hypergraph.

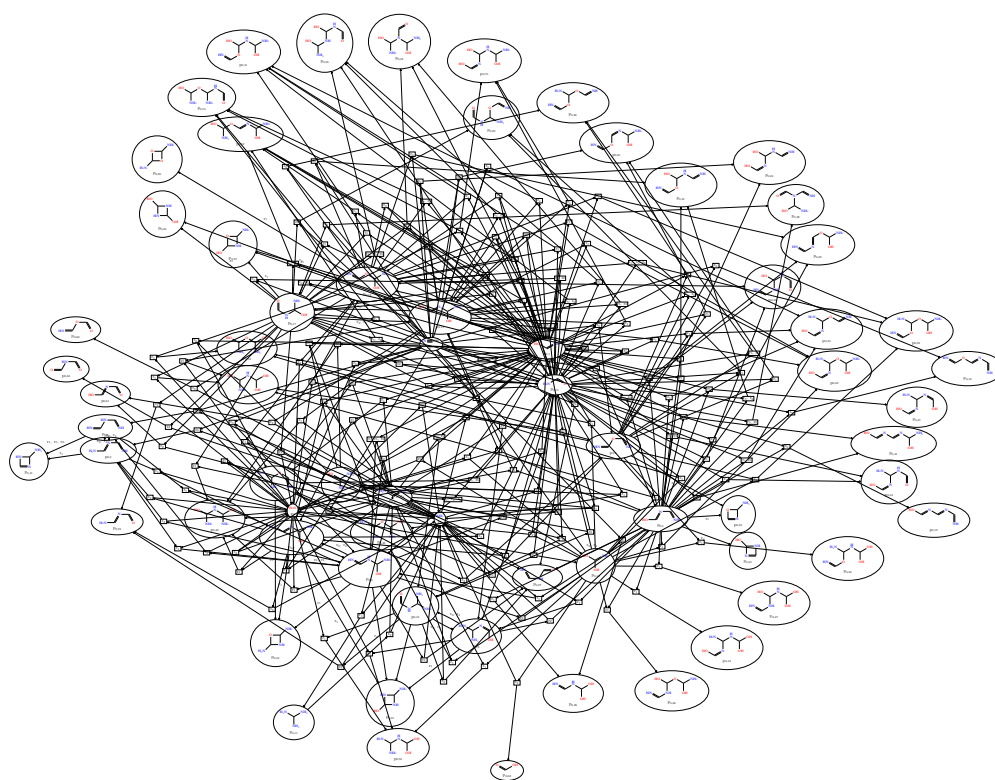


FIG. 9. Hypergraph with $|V| = 67$ and $|E| = 202$, representing the reaction network considered in this work, provided here for the sake of completeness.